INTERFACE SCIENCE 1, 7–30 (1993).

Interfacial Segregation in Ag-Au, Au-Pd, and Cu-Ni Alloys: I. (100) Surfaces

H.Y. WANG, R. NAJAFABADI, AND D.J. SROLOVITZ
Department of Materials Science and Engineering, University of Michigan, Ann Arbor, MI 48109

R. LESAR
Theoretical Division, Los Alamos National Laboratory, Los Alamos, NM 87545

Received August 9, 1992; Revised December 15, 1992.

Keywords: Surfaces, computer simulation, free energy, segregation.

Abstract. Atomistic simulations of segregation to (100) free surface in Ag-Au, Au-Pd, and Cu-Ni alloy systems have been performed for a wide range of temperatures and compositions within the solid solution region of these alloy phase diagrams. In addition to the surface segregation profiles, surface free energies, enthalpies, and entropies were determined. These simulations were performed within the framework of the free energy simulation method, in which an approximate free energy functional is minimized with respect to atomic coordinates and atomic site occupation. The effects of the relaxation with respect to either the atomic positions or the atomic concentrations are discussed. For all alloy bulk compositions ($0.05 \leq C \leq 0.95$) and temperatures ($400 \leq T(\mathrm{K}) \leq 1,100$) examined, Ag, Au, and Cu segregates to the surface in the Ag-Au, Au-Pd, and Cu-Ni alloy systems, respectively. The present results are compared with several theories for segregation. The resultant segregation profiles in Au-Pd and Ag-Au alloys are shown to be in good agreement with an empirical segregation theory, while in Cu-Ni alloys the disagreement in Ni-rich alloys is substantial. The width of the segregation profile is limited to approximately three to four atomic planes. The surface thermodynamic properties depend sensitively on the magnitude of the surface segregation, and some of them are shown to vary linearly with the magnitude of the surface segregation.

1. Introduction

Alloying elements and impurities often segregate to the surface or near-surface region of a solid. Since many material properties depend on surface properties, segregation plays an important role in such diverse phenomena as: catalysis, chemisorption, corrosion, thermionic emission, crystal growth, etc. Therefore, an understanding of these surface phenomena requires a knowledge of not only the structure of the surface, but also of the surface composition. The surface composition, in turn, depends on the surface segregation thermodynamics. The focus of the present work is the application of the recently introduced, free-energy simulation method [1–4] to the determination of the equilibrium structure, composition, and thermodynamics of alloy surfaces. In particular, the present paper examines (100) surfaces in Ag-Au, Au-Pd, and Cu-Ni alloys. The segregation profiles and the related thermodynamic properties in these three alloy systems are determined, and the agreement between the present results and several segregation theories are discussed.

A century ago, Gibbs [5] predicted that one of the components of an alloy will segregate to a surface if the surface tension decreases

when the surface concentration of that component increases. Unfortunately, very little is known about the composition dependence of the surface energy. Therefore, many alternative approaches for predicting surface segregation have been suggested [6–8]. Thirty-five years ago, McLean [9] proposed a segregation model which is a variant of Langmuir's classical surface adsorption isotherm and is valid for both segregation to grain boundaries and free surfaces. This model reduces to the following prediction:

$$\frac{C_1}{1-C_1} = \frac{C_B}{1-C_B}\exp\left(-\frac{\Delta G}{kT}\right) \tag{1}$$

where C_1 is the interfacial concentration of the impurity or solute; C_B is the bulk solute concentration; and ΔG is the partial atomic excess free energy of segregation or the heat of segregation, and is taken as a *constant*. This expression ignores all interactions between impurity atoms, and limits the interfacial segregation to a single atomic plane consisting of equivalent atomic sites. These restrictions suggest that equation (1) is only approximate and is most appropriate for dilute interfacial and bulk concentrations.

McLean further estimated the driving force for adsorption as the strain energy of the solute in the bulk. This assumes that the strain energy induced by the size difference between solute and solvent would be eliminated completely by the exchange of a solute atom in the bulk with a solvent atom at the surface. With such an assumption, solute segregation to the surface will always occur. This, of course, cannot explain several experimental observations in which the surface becomes enriched in solvent atoms.

In contrast to the McLean approach, Defay [10] estimated the heat of segregation (initially for surface segregation of liquid solution, but also valid for solid solutions) by evaluating the change in the number of nearest neighbor bonds that occurs when an atom of the segregating species, located in the bulk, exchanges positions with an atom of the other species, located at the surface. This method (known as a regular solution, lattice gas, or bond-breaking model) was later extended to include four distinct surface layers by Williams and Nason [11]. For a monolayer surface model, this leads to the following heat of segregation:

$$\Delta G = \frac{Z_v}{Z}\Delta H_{\text{sub}} + 2\omega\left(ZC_B - Z_1C_1 - Z_vC_B - \frac{1}{2}Z_v\right) \tag{2}$$

where ΔH_{sub} is related to the difference between the sublimation energies of A and B atoms: ω is the regular solution parameter defined as $\varepsilon_{AB} - 0.5(\varepsilon_{AA} + \varepsilon_{BB})$; ε_{AB}, ε_{AA}, ε_{BB} are the nearest neighbor interaction energies between $A-B$, $A-A$, and $B-B$ nearest neighbor bonds, respectively; Z_1, Z_v, and Z are the number of lateral surface bonds, vertical surface bonds (i.e., bonds broken when the surface is formed), and perfect crystal nearest neighbors bonds, respectively. Although the equivalent bond treatment for the bulk and the surface makes the model simple to apply, it unfortunately overestimates the degree of segregation [11–14]. In a further extension, an empirical parameter δd is introduced, which accounts for the change in bond energy due to surface relaxation. This leads to

$$\Delta G = \left[\Delta H_{\text{sub}}\frac{[Z_v - (Z_1 + Z_v)\delta]}{Z} + 2\omega\left(ZC_B - (1+\delta)(Z_1C_1 + Z_vC_B) + \frac{\delta}{2}Z_1 + \frac{\delta-1}{2}Z_v\right)\right] \tag{3}$$

It was shown that when δ is chosen optimally, equation (3) leads to accurate segregation predictions [12, 14, 15]. Unfortunately, δ can only be obtained by fitting to experiment data. According to the bond-breaking models, the component having the lower heat of sublimation will always segregate to the surface, which contradicts experimental observation of segregation of minority species with higher binding energies in very dilute alloys.

Wynblatt and Ku [16] replaced the sublimation energy term in equation (2) with the difference of surface energy of the two elements (solute and solvent), and calculated the regular solution parameter from the heat of mixing. In this model, the heat of segregation is given as

$$\Delta G = \Delta(\gamma\sigma) + 2\omega\left(ZC_B - Z_1C_1 - Z_vC_B - \frac{1}{2}Z_v\right) \quad (4)$$

where γ and σ are the surface energy and surface area per atom in the pure systems. Surface relaxation is automatically taken account of in the surface free energy difference term in equation (4). In light of the deficiencies of both the strain energy and the bond-breaking models, Wynblatt and Ku [16] argued that the total system free energy should include the contributions from both bond and strain energies and combined them as the sum of two independent terms. They determined the bond-energy contribution from equation (4) and the strain-energy contribution from Friedel's elastic misfit analysis [17]

$$E_{el} = -\frac{24PK_AG_Br_Ar_B(r_A - r_B)^2}{3K_Ar_A + 4G_Br_B} \quad (5)$$

where K_A is the bulk modulus of pure A (A is the solute); G_B is the shear modulus of pure B; and r_A and r_B are the atomic radii of pure A and pure B, respectively. Although, this model works reasonably well for dilute cases and can be modified to describe ordered binary alloy surfaces [18], the validity of the assumptions of linear elasticity and the complete release of the strain energy on segregation may be questionable.

Abraham et al. [19–21] used Lennard-Jones pair potentials and Monte Carlo simulations to determine the heat of segregation. They defined the boundary separating the solute and solvent segregation regions in the ε^*--σ^* and γ^*--σ^* spaces by determining the value ε^*, γ^*, and σ^* at the zero segregation heat, where ε^*, γ^*, and σ^* are the bond-strength ratio, surface-energy ratio, and the atomic-size ratio, respectively. The effects of bond strength and atomic size difference were automatically included, and these authors demonstrated that the linear elastic treatment of the strain energy overestimates the strain-energy decrease (especially for the case where the solute atom has a smaller size than the solvent atom). They also found that large solute atoms had greater tendencies to segregate than did small atoms, since the lattice distortion was more pronounced for oversized atoms. Although the theory, which they derived based upon the simulation results, successfully predicted which element would segregate in about 85% of the cases examined, it was not designed to quantitatively evaluate the magnitude of the segregation and is only applicable in dilute cases.

An alternative approach for determining which element will segregate was suggested by Burton and Machlin [22]. Observing that a solid surface differs from the bulk in characteristics similar to those of a liquid (such as lower symmetry, lower coordination, and no elastic strain), they suggested that the solute should segregate if the solid-liquid equilibrium is such that the liquid is richer in solute and the separation between the solidus and the liquidus is large. They were able to show that most of the experiment results could be rationalized with this concept. Unfortunately, this type of criterion is not able to predict the degree of surface segregation, and it does not specify how large the separation between the solidus and the liquidus must be in order for a segregation to occur.

A different approach for predicting segregation behavior was developed by Strohl and King [23, 24] who derived a multilayer and multi component surface segregation model based upon a rigorous thermodynamic approach. The concentration of species i at layer number n is given as

$$C_i^n = \left[\frac{za_i^B}{z_1\gamma_i^n + z_v(\gamma_i^{n-1} + \gamma_i^{n+1})}\right] \times \exp\left(\frac{\overline{A}_i^n\sigma^n - A_i^n\sigma^n}{RT}\right) \quad (6)$$

where a_i^B is the activity of i in the bulk; γ_i^n, γ_i^{n-1}, and γ_i^{n+1} are the activity coefficients of i associated with layer n, $n-1$, and $n+1$; $\overline{A}_i^n$ and A_i^n are the partial molar area of i in layer n and the molar area of pure i in layer n; and σ^n and σ_i^n are the surface free energy associated with layer n and the surface free energy of pure i in layer n. The surface relaxation is partially accounted for in the surface energy terms, and unlike the other regular solution models, the mixing behavior can be nonregular such that short range order may be included. Comparison of these results with Monte Carlo data [23, 24] show good agreement, however, this

model does not explicitly include strain-energy effects.

Recent advances in Monte Carlo atomistic simulation methods [25–29] have enabled this simulation approach to be extended to alloy systems where the local composition can change during the course of the simulation. This has led to truly atomistic studies of equilibrium segregation to interfaces that do not rely on the classical theories. Although this method does yield equilibrium interfacial structure and composition, it has never been successfully used to obtain information about such basic segregation thermodynamic properties as the free energy of segregation. In addition, these calculations require very substantial computational resources.

The recently introduced free energy minimization method [1–4], on the other hand, is computationally efficient, and yields segregation results that are in excellent agreement with Monte Carlo data. Although this approach is inherently less accurate than the Monte Carlo method, its efficiency allows systematic evaluations of trends in interfacial and segregation thermodynamics as a function of experimental parameters such as temperature and bulk composition. The most important feature of this method is that it yields a simple expression for the finite-temperature free energy of the system. Minimizing the free energy with respect to the positions and concentrations of the atomic sites yields equilibrium segregation profiles, atomic structures, and free energies, from which all other thermodynamic quantities may be derived.

The present paper focuses on the application of this free energy simulation method to (100) surface segregation in three alloy systems: Ag-Au, Au-Pd, and Cu-Ni. These three systems were chosen because they represent cases where the atomic size mismatch and sublimation energies vary over an appreciable range. The degree of segregation and the segregation thermodynamics are predicted over a wide range of temperature and alloy compositions. The present results are compared with several theories for segregation.

2. Method

In this section, we briefly outline the free energy simulation method, which we employ to determine the equilibrium structure, composition and thermodynamics of surfaces in alloys. A more complete description may be found elsewhere [1–4]. We construct an approximate free energy functional for a multicomponent atomic system and then minimize it with respect to the atomic coordinates and the compositional profile in the material. The free energy of a multicomponent system consists of several distinguishable parts, including atomic bonding, atomic vibrations and configurational entropy (i.e., the entropy associated with the relative spatial distribution of the atomic species). For the metallic systems examined in the present study, we describe the atomic interactions within the framework of the embedded atom method (EAM) [30–32]. The effects of atomic vibrations are included within the framework of the local harmonic (LH) model [33]

$$A_v = k_B T \sum_{i=1}^{N} \sum_{\beta=1}^{3} \ln\left(\frac{h\omega_{i\beta}}{2\pi k_B T}\right) \tag{7}$$

where A_v is the vibrational contribution to the free energy; k_BT is the thermal energy; h is Planck's constant; N is the total number of atoms in the system; and ω_{i1}, ω_{i2}, and ω_{i3} are the three vibrational eigenfrequencies of atom i. These frequencies may be determined in terms of the local dynamical matrix of each atom $D_{iab} = (\partial^2 E/\partial x_{ia}\partial x_{ib})$, where E is the potential energy determined from the interatomic potential, and x_{ib} corresponds to atomic displacements of atom i in the b direction. Diagonalization of this 3×3 matrix yields the three force constants k_{ib} for atom i. The vibrational frequencies are then determined as $\omega_{ib} = (k_{ib}/m)^{1/2}$, where m is the effective atomic mass. We have demonstrated that the approximations inherent in the LH model lead to errors in the free energy of perfect close-packed metal crystals of the order of 1% at the melting temperature and much less at lower temperatures [33, 34].

Configurational entropy S_c is described on the

basis of a point approximation:

$$S_c = -k_B \sum_{i=1}^{N} \{c_a(i) \ln[c_a(i)] + c_b(i) \ln[c_b(i)]\} \tag{8}$$

where $c_a(i)$ is the concentration of **a** atoms and $c_b(i)$ is the concentration of **b** atoms on site i. Since we are interested in equilibrium properties, these concentrations may be viewed as the time-averaged composition of each atomic site in a system where the atoms are free to diffuse. In this sense, the atoms are "effective" or "mean-field" atoms. Since we replace real atoms by effective atoms, the internal energy E, which is defined in terms of the interatomic potential, must also be suitably averaged over the composition of each atom and its interacting neighbors. A method for performing these averages for the EAM potentials is described [1–4]. The point approximation for the configurational entropy and the mean-field treatment for each atomic site, like the regular solution models described above, do not accurately account for short-range order effects. However, it was demonstrated by Kumar [13, 14] that the effect of short-range order is not important in determining the degree of segregation.

The present simulations were performed within a reduced grand canonical ensemble, where the total number of atoms remains fixed but the relative quantities of each atomic species varies. The appropriate thermodynamic potential for this type of ensemble is the grand potential and is given by [35]

$$\Omega = E + A_v - TS_c - \Delta\mu \sum_{i=1}^{N} c_a(i) \tag{9}$$

where $\Delta\mu$ is the difference in chemical potential between the **a** and **b** atoms and E is the static lattice energy.

The equilibrium surface segregation profile is determined in several steps. First, the properties of the perfect, uniform composition crystal are determined (see the Appendix). This is done by choosing a composition and then minimizing the Gibbs free energy, at the temperature and pressure of interest, with respect to the lattice parameter. Differentiating this equilibrium free energy with respect to composition gives the chemical potential difference $\Delta\mu$. Since, at equilibrium, the chemical potential of a component is everywhere constant, we fix the chemical potential differences at their bulk values, introduce the appropriate surface, and minimize the grand potential with respect to the concentration and position of each atomic site.

Although the free energy functional that we employ is approximate, it has been shown to produce results that are in good agreement with Monte Carlo data obtained using the same potential [1]. Nonetheless, these approximations can lead to significant errors near critical points in the phase diagram. Therefore, this approach should be applied with caution in these regions of the phase diagram. The results presented in this study were all performed under conditions far from the critical points.

The geometry of the cell used in the surface simulations is divided into two regions: I and II. The surface is located in the region I and the atoms in region I are completely free to move in response to the forces due to other atoms, and the concentration at each site is allowed to vary. The atoms in region II, however, are constrained such that region II is a perfect crystal with the lattice constant and average concentration on each site appropriate to the simulation temperature, pressure, and bulk concentration. The equilibrium atomic configuration and the concentration of each effective atom are obtained by minimizing equation (9) with respect to the atomic coordinates and the site concentrations ($4N$ variables, where N is the number of atoms in the system). In the direction of the surface normal (i.e., the z-direction), there are no constraints imposed on the particles, such that the traction in z-direction is guaranteed zero. The simulations were performed with a total of 20 atoms in each of the (002) planes in the simulation cell. Typically, eight (002) planes were required in order to obtain surface energies that were invariant with respect to increasing the number of planes in the simulation cell. The conjugate gradient method [36] is used to minimize the grand potential, and the procedure is stopped when the magnitude of the gradient of the grand potential is less than $10^{-4} eV/Å$ (typically $10^{-5} eV/Å$).

3. Results

Simulations based upon the free energy simulation method were performed on (100) surfaces in Ag-Au, Au-Pd, and Cu-Ni alloys for temperatures between 400 and 1,100 K. At each temperature, between 13 and 19 different bulk compositions were examined. The temperatures and compositions examined in this study are all within the continuous solid solution region of the phase diagrams of the three alloys, as determined from perfect crystal free energy simulation results using the same EAM potentials [32]. We note that the EAM potentials used in the present study are different than the EAM potentials [25] we used in our previous study of interfacial segregation in Cu-Ni system [1]. This leads to some differences in the computed segregation profile.

The thermodynamic properties of the surfaces are distinguished from the bulk properties by the subscripts B or s, where B represents bulk, (solid solution) crystal properties; and s refers to surface properties. The surface properties are defined as the difference between the property of the system containing the surface and that of a solid solution crystal with the same number of atoms at the same bulk composition and temperature $X_s = [X(\text{surface}) - X_B]/A$, where X is the thermodynamic property of interest (e.g., free energy, enthalpy, etc.), and the surface properties have been normalized by the surface area A. The surface properties may be calculated in two limits. The first is the unsegregated limit, as may be found by rapidly quenching the sample from very high temperature (where segregation is negligible) to the temperature of interest, and its properties are denoted by $X_{s,u}$. The second limit corresponds to equilibrium segregation at the temperature of interest and is denoted by $X_{s,s}$. The change in the thermodynamic properties that may be associated with the segregation is given by the difference between these two values, i.e., $\Delta X_s = X_{s,s} - X_{s,u}$.

The dimensionless concentrations (or fractions of (002) monolayers) on the (002) planes parallel to the surface are given by C_n, where the subscript n denotes the plane number (e.g., C_3 is the concentration on the third (002) plane from the surface). Throughout this paper, all concentrations $0 \leq C \leq 1$ will refer to the Ag concentration for Ag-Au alloys, Au for Au-Pd, and Cu for Cu-Ni alloys; the concentrations for the other components of these binary alloys are given simply by $1 - C$. The degree of segregation, or *excess* concentration, is defined as the difference between the concentration on the plane and the bulk concentration and is denoted $C_{n,xs} = C_n - C_B$. The net, or *total excess* segregation is the sum of $C_{n,xs}$ over all (002) planes and is referred to as $C_{T,xs} = \sum_{n=1}^{\infty} C_{n,xs}$. $C_{T,xs}$ is nonzero here, since the present simulations were performed in the grand canonical ensemble, while in either the canonical or microcanonical ensemble $C_{T,xs} = 0$.

3.1. Segregation Profiles

The concentration profiles in the vicinity of the (100) surface for Ag-Au, Au-Pd, and Cu-Ni alloys are shown in figure 1 at $T = 600$ K and different bulk concentrations C_B. When the bulk concentration C_B is varied from 20% to 80% Cu in the Cu-Ni system, the Cu concentration at the surface ($n = 1$) varies over a small range (82% to 97%). The second (002) plane from the surface ($n = 2$) exhibits Ni segregation and the magnitude of the Ni segregation is much less than the Cu segregation to the first (002) plane. The third (002) plane also shows Ni segregation of even smaller magnitude. By the fourth (002) plane from the surface, the Cu concentration is nearly equal to the bulk concentration. These segregation profiles indicate that the effective width of the free surface segregation profile is approximately three (002) planes, and that the total excess concentration $C_{T,xs}$ for C_B less than about 0.5 is dominated by $C_{1,xs}$. When C_B is larger than 0.5, however, the contribution from the second layer is quite significant.

In the Au-Pd alloys (Fig. 1(*b*)), the concentration profile exhibits a different form than that seen in the Cu-Ni alloys. When the bulk concentration of Au increases from 20% to 80%, the first two (002) planes are enriched in Au, although the second plane shows a much smaller degree of Au segregation. On the third plane, however, the Pd concentration is enriched, but by the fourth plane the Au concentration is en-

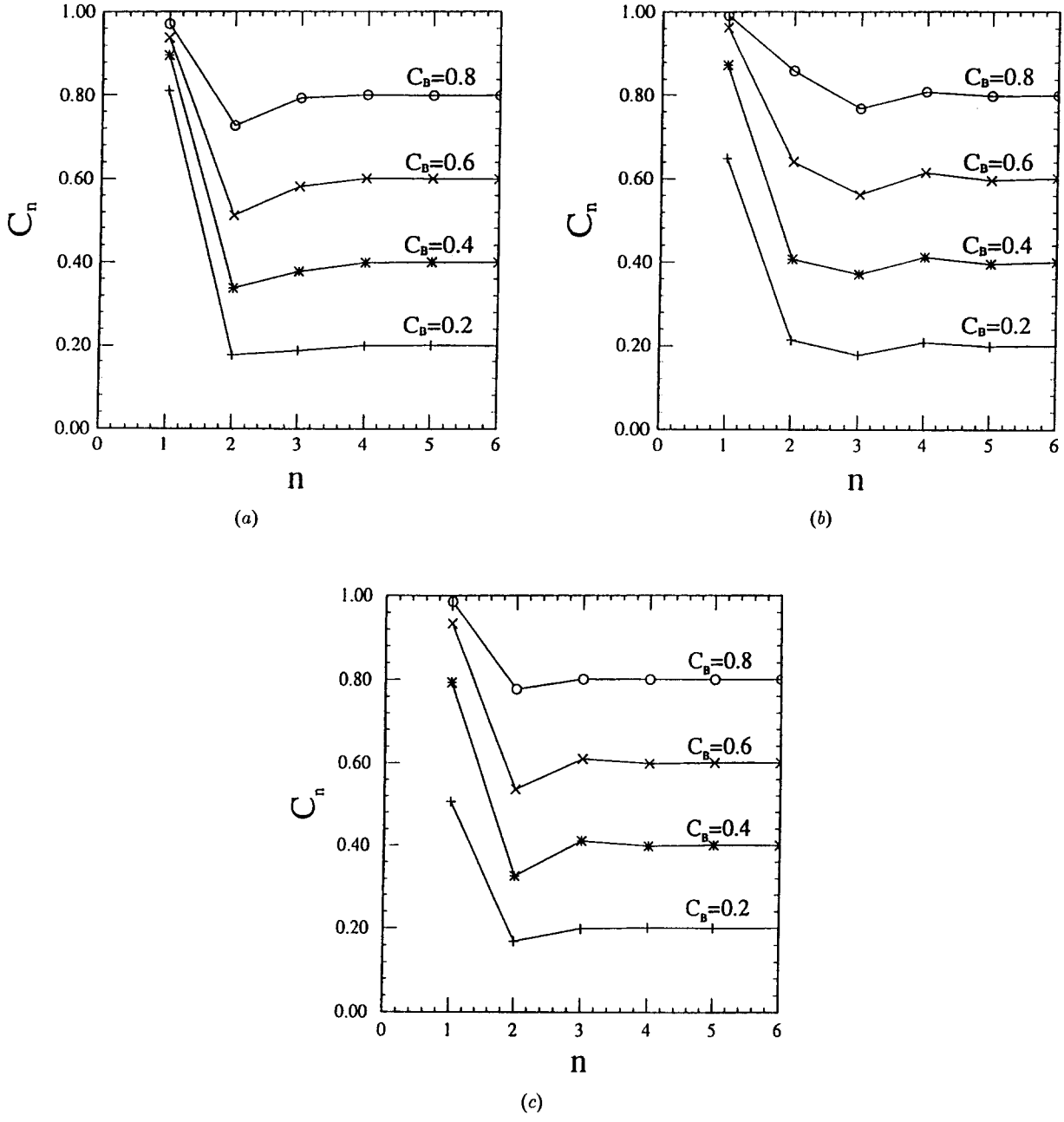

Fig. 1. Concentration C_n (002) planes parallel to the surface versus layer number n where $n = 1$ corresponds to the (002) plane adjacent to the surface with (*a*) for the Cu-Ni; (*b*) for Au-Pd; and (*c*) for Ag-Au alloys. The temperature is 600 K.

riched again. The effective width of the surface segregation profile is somewhat larger than in the Cu-Ni system (about 4 (002) planes). The main difference between the shape of the concentration profiles in Cu-Ni and Au-Pd alloys is that the change in segregant occurs at the second layer in Cu-Ni alloys and not until the third layer in Au-Pd alloys. In the Ag-Au system (Fig. 1(*c*)), the segregation pattern is similar to that of Cu-Ni alloys: the oscillation occurs at the second layer, however, the magnitude of the segregation and the decay length of the concentration profile are smaller in Ag-Au than in Cu-Ni alloys.

The effects of temperature and bulk concentration on the first-layer segregation may be seen more clearly in figure 2, where we plot C_1 as a function of the bulk concentration for different temperatures. In this type of plot, the straight line $C_1 = C_B$ corresponds to zero segregation. Clearly, $C_1 = 0$ in the limit that C_B goes to zero and C_1 must go to unity as C_B approaches one since in these limits no solute is present. In all three systems, the same element segregates for all T and C_B examined (Cu in Cu-Ni, Au in Au-Pd, and Ag in Ag-Au). Cu-Ni alloys exhibit stronger segregation than Au-Pd, and both show stronger segregation than occurs in Ag-Au alloys. The main effect of increasing temperature is simply to reduce the magnitude of the segregation.

The magnitude of the segregation in the three alloy systems may be seen more clearly in figure 3 where we plot the excess concentration of the surface plane as a function of the bulk concentration at $T = 600$ K. In this kind of plot, $C_{1,xs}$ must go to zero as the bulk concentration goes to zero or one. The maximum degree of Cu segregation in Cu-Ni is ~ 0.6 at $C_B = 0.16$, ~ 0.5 at $C_B = 0.3$ for Au in Au-Pd, and ~ 0.4 at $C_B = 0.4$ for Ag in Ag-Au. We see that as the maximum degree of segregation decreases, the bulk concentration at which the surface concentration maximum occurs approaches 0.5. This is undoubtedly associated with the increased importance of the configurational entropy (which favor 50% composition) as the strength of the other terms in the free energy, which favor segregation decrease.

3.2. Surface Free Energy

All of the surface thermodynamic properties are defined as the difference between those properties in the system with the surface and that of the bulk (see Appendix) and normalized by the area of the surface, as described above. The surface free energy in the grand canonical ensemble, is denoted as $G_s = (\Omega_s - \Omega)/A$, where Ω_s is the grand potential of the system with the surface, Ω is the grand potential for the perfect crystal, and A is the area of the surface. G_s is plotted as a function of bulk concentration C_B in figure 4 both with (solid curves) and without (dotted curves) segregation. When segregation is allowed to occur, the grand potential is minimized with respect to the position and the concentration of each site, while for the unsegregated surface, the compositions of each site are fixed at C_B and the grand potential is minimized only with respect to the atomic coordinates. In all three alloy systems, the unsegregated surface free energy $G_{s,u}$ varies in a nearly linear manner with the bulk concentration C_B. The $G_{s,u}$ versus C_B are well approximated by linear interpolations between the G_s values of the two pure elements in the alloys and the effect of increasing temperature is simply to shift these curves to lower values of G_s. This temperature dependence implies a positive surface entropy.

The G_s versus C_B curves for the segregated surfaces are much more complicated than in the unsegregated case. The complexity is introduced by the competition between the various terms that make up the free energy: enthalpy, entropy, and chemical potential. The lower the temperature, the smaller the entropic contribution to the free energy, such that $G_{s,s}$ is larger. However, since segregation is more pronounced at lower temperatures, the larger the contribution from the energy that drives segregation, and, hence, the smaller the magnitude of $G_{s,s}$.

For bulk Cu concentrations less than approximately 0.5 in the Cu-Ni alloys (Fig. 4(*a*)), $G_{s,s}$ is smallest at the lowest temperature studied ($T = 400$°K). For $C_B > 0.5$, the smallest surface free energy is found at the highest temperature studied ($T = 1{,}000$°K). These results may be

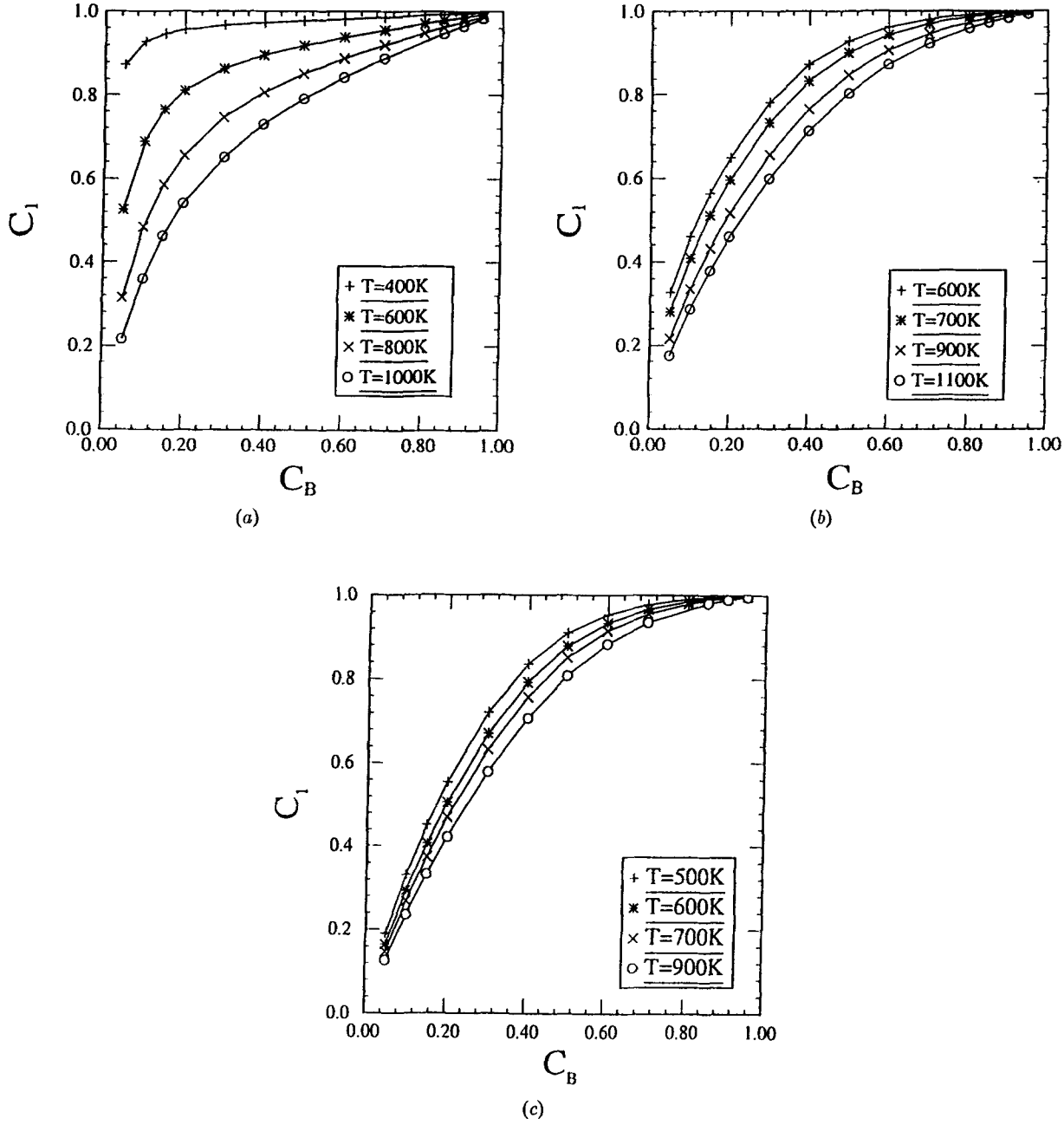

Fig. 2. The concentration of the first (002) plane C_1 is plotted as a function of the bulk concentration C_B and (*a*), (*b*), and (*c*) are for the Cu-Ni, Au-Pd, and Ag-Au alloys, respectively.

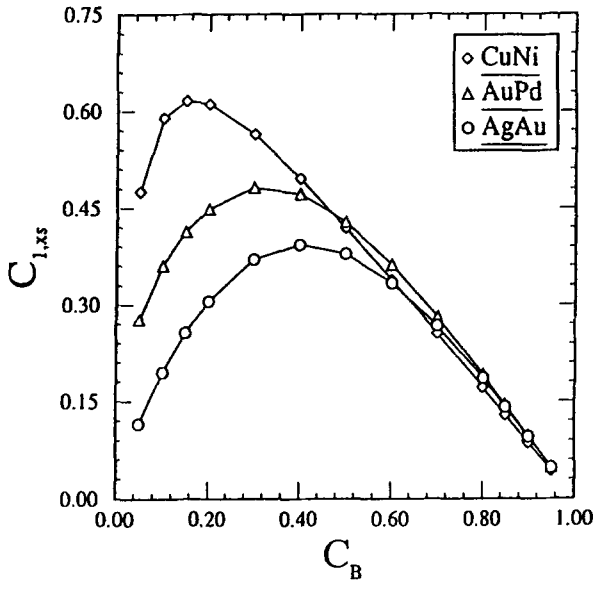

Fig. 3. The excess concentration of the first (002) plane versus bulk concentration C_B with temperature 600 K. The diamond, triangle, and circle are for Ag-Au, Au-Pd, and Cu-Ni alloys, respectively.

understood by considering the effects of bulk concentration and temperature on the segregation behavior (see figure 2). The degree of Cu segregation is greatest at low temperatures and for bulk concentrations on the Ni-rich side of the phase diagram. In this regime (low T, small C_B), where the degree of segregation is a maximum, $G_{s,s}$ is a minimum. On the other hand, at high T and large C_B, the degree of segregation is small. In this regime, the ordering of the different temperature curves in the $G_{s,s}$ versus C_B plot are as they are in the absence of segregation.

In Au-Pd and Ag-Au alloys (Fig. 4(*b*) and (*c*)), the segregation is not as strong as that in the Cu-Ni alloys, implying that the segregated surface free energy curves will vary simply with C_B and T as in the unsegregated case. Although the decrease in the surface free energy curves from the unsegregated $G_{s,u}$ to segregated $G_{s,s}$ cases varies with temperature, the ordering of the $G_{s,u}$ curves with temperature are still retained upon segregation. This suggests that in all three cases, the shape of the free energy curves are dominated by the internal energy.

4. Discussion

In the previous section, we reported results on segregation to the (100) free surface in Ag-Au, Au-Pd, and Cu-Ni alloys as a function of both temperature and composition. We noted that there is a correlation between the excess concentration and the change of the surface free energy from segregated surfaces to unsegregated surfaces. To investigate the nature of the correlations between segregation and surface properties, we focus on that part of the thermodynamic properties that depends on the segregation per se; that is, the difference between the thermodynamic properties with and without segregation. It is important to focus on this difference so as not to bias the results with intrinsic properties of the surface (e.g., the surface vibrational entropy varies as C_B goes from zero to one even without segregation). We begin by examining these excess properties as a function of the total excess concentration.

For Cu-Ni alloys, figure 5(*a*) shows the excess vibrational entropy, $\Delta S_{s,v}$, as a function of the total excess concentration $C_{T,xs}$. Similarly, Fig. 5(*b*) and Fig. 5(*c*) show the excess enthalpy ΔH_s and the change in separation between the first two (002) planes upon segregation $\Delta d_{1,2}$ as a function of $C_{T,xs}$. These plots consist of data taken over the entire range of temperature and concentration reported in the previous section. In all three cases, we find that there is a linear relationship between these surface thermodynamic properties and the total excess concentration. Linear numerical fits to this data yield $\Delta X_s = m C_{T,xs}$ with the slope $m = 0.190 \pm 0.002\ mJ/m^2K$ for $\Delta S_{s,v}$, $m = 1956 \pm 14\ mJ/m^2$ for ΔH_s, and $m = 0.0367 \pm 0.0004$ Å for $\Delta d_{1,2}$. The configurational contribution to the excess surface entropy $\Delta S_{s,c}$ does not exhibit a linear dependence on $C_{T,xs}$ due to the explicitly prescribed nature of the configurational entropy (Eq. 8). The excess surface grand potential ΔG_s is an approximately linear function of $C_{T,xs}$. However, due to the presence of the $\Delta S_{s,c}$ term, there is considerably more scatter than for $\Delta S_{s,v}$, ΔH_s, and $\Delta d_{1,2}$.

For Au-Pd alloys, the excess vibrational entropy, $\Delta S_{s,v}$, the excess separation between the

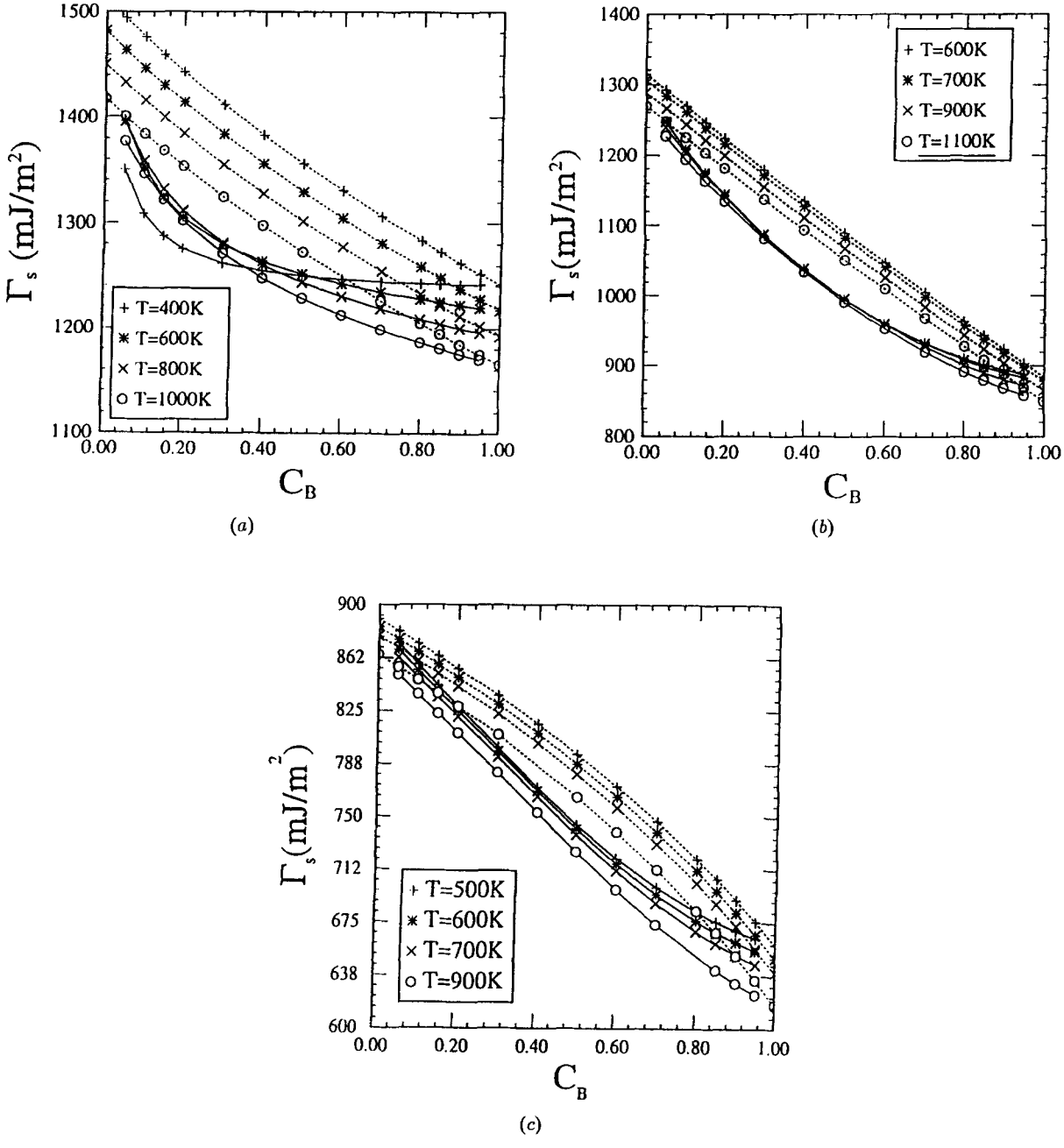

Fig. 4. The surface free energy is plotted as a function of the bulk concentration with four different temperatures and (*a*), (*b*), and (*c*) are for Cu-Ni, Au-Pd, and Ag-Au alloys, respectively. The solid lines are for the segregated boundary, and the dashed lines are for the unsegregated boundary.

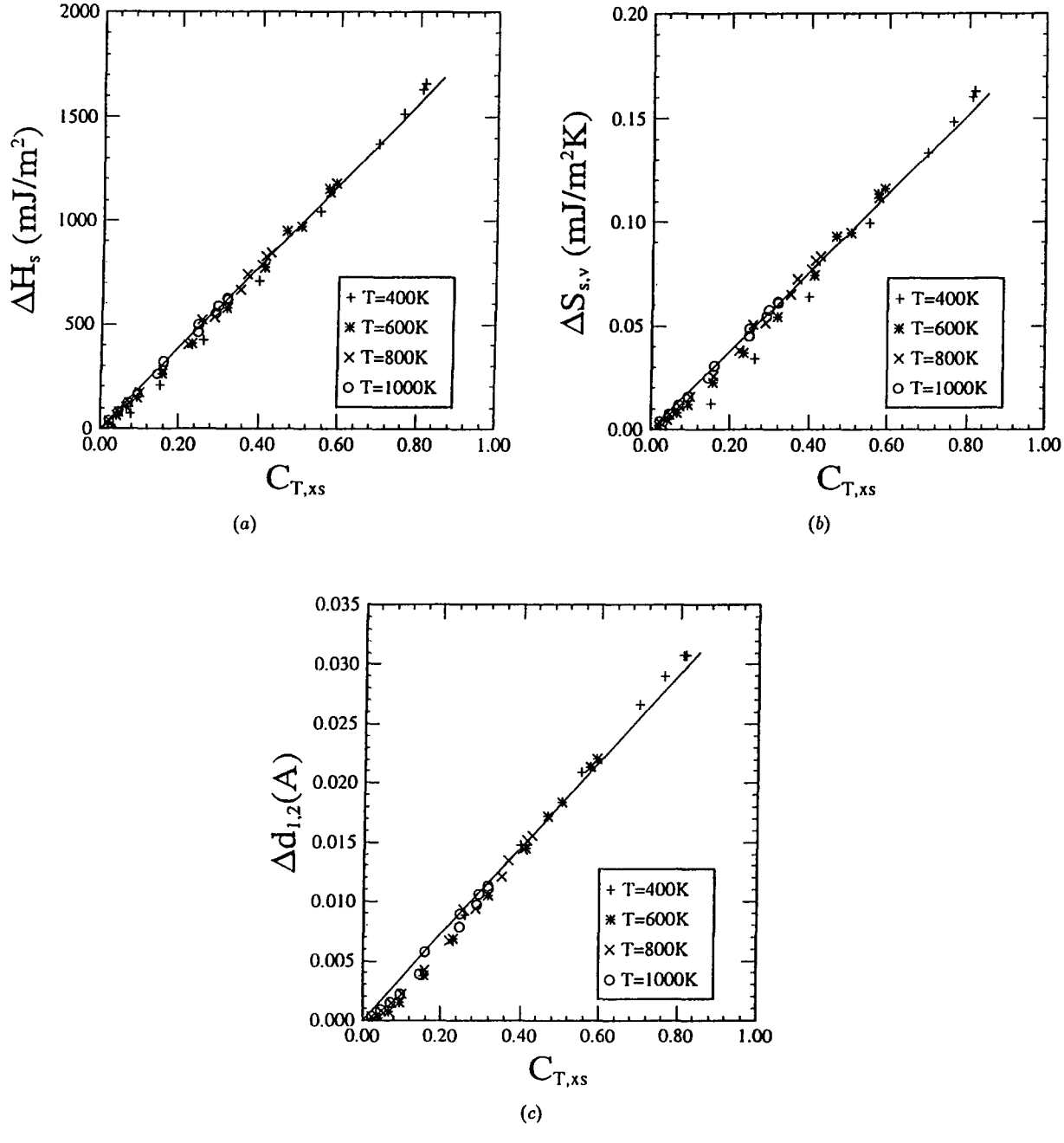

Fig. 5. (*a*) The excess surface vibrational entropy, (*b*) excess surface enthalpy, and (*c*) excess separation between the first two (002) planes of Cu-Ni alloys versus the total excess concentration. The straight lines are fit to all of the data.

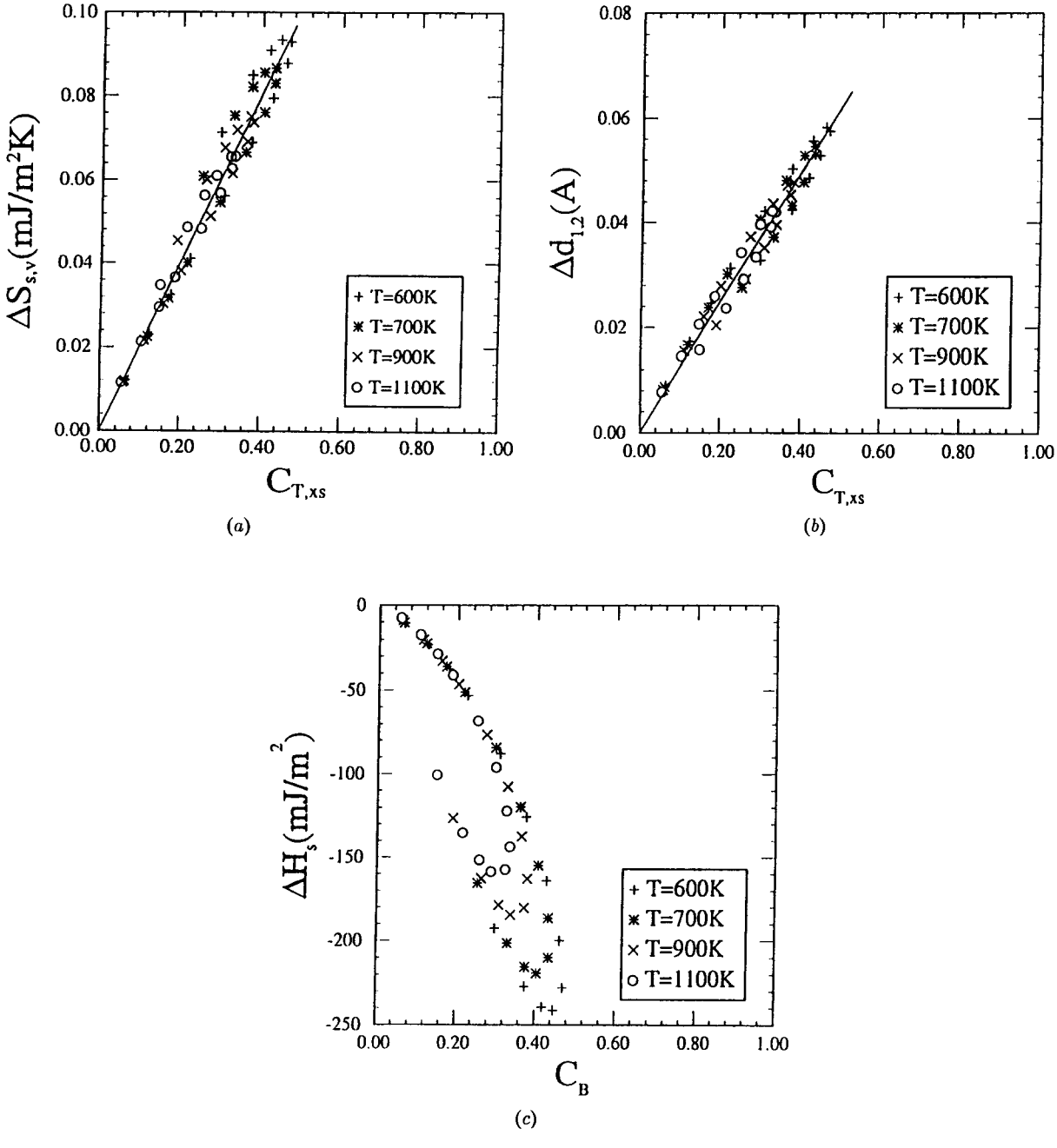

Fig. 6. (*a*) The excess surface vibrational entropy, (*b*) excess separation between the first two (002) planes, and (*c*) excess surface enthalpy of Au-Pd alloys versus the total excess concentration. The straight lines are fit to all of the data.

first two planes $\Delta d_{1,2}$, and the excess enthalpy, ΔH_s are plotted as functions of the total excess concentration $C_{T,xs}$ in figure 6. As in the Cu-Ni alloy system, the excess vibrational entropy and change in the separation between the first two planes upon segregation are linear functions of the total excess concentration for all C_B and T. If we fit these data to a linear equation $\Delta X_{gb} = mC_{T,xs}$, we find $m = 0.201 \pm 0.002\ mJ/m^2K$ for $(\Delta)DS_{s,v}$, and $m = 0.124 \pm 0.001$ Å for $(\Delta)Dd_{1,2}$. Because Au has a larger (100) surface entropy and atomic size than that for Pd, the values of $\Delta S_{s,v}$ and $\Delta d_{1,2}$ are positive when Au segregates. The excess enthalpy data shows a much wider scatter band than was observed in Cu-Ni. The main effect may be attributed to the pronounced nonlinear relationship in the Au-Pd enthalpy versus bulk composition plot (Fig. A3(*b*) as compared with the linear relationship between H and C_B for Cu-Ni crystals. This implies that the interaction between Au and Pd atoms is quite different from that between Cu and Ni atoms. This is consistent with the fact that Au-Pd exhibits a regular solution parameter w which is of largest magnitude among the three alloys systems examined here ($\omega_{\text{Au-Pd}} = -0.01$, $\omega_{\text{Cu-Ni}} = 0.005$, and $\omega_{\text{Ag-Au}} = -0.009$—see below). Therefore, Cu-Ni and Ag-Au alloys should be expected to show a better linear dependence between the excess enthalpy and the excess concentration than Au-Pd alloys, as borne out in figures 5(*b*), 6(*c*) and 7(*a*).

The excess enthalpy ΔH_s, and the change in separation between the first two planes upon segregation $\Delta d_{1,2}$, are plotted as functions of the total excess concentration $C_{T,xs}$, in figure 7(*a*) and 7 (*b*) for Ag-Au alloys. As mentioned above, ΔH_s exhibits a good linear correlation with the excess concentration. Although the data for $\Delta d_{1,2}$ shows some scatter, $\Delta d_{1,2}$ may reasonably be described as varying linearly with $C_{T,xs}$. If we fit these data to a linear equation, $\Delta X_{gb} = mC_{T,xs}$, we find $m = 1887 \pm 7.28\ mJ/m^2$ for ΔH_s and 0.138 ± 0.002 Å for $\Delta d_{1,2}$.

As described above, all of the equilibrium surfaces were obtained by minimizing the grand potential Ω (Eq. (9)) with respect to the position and the concentration of each site in the system. Taking the derivative of the equilibrium grand potential, Ω, with respect to the concentration of plane n, yields an analytical expression for determining the concentration on plane n:

$$\frac{C_n}{1-C_n} = \frac{C_B}{1-C_B} \times \exp\left[\left(\frac{\partial F}{\partial C_n} - \frac{\partial F}{\partial C_B}\right)/kT\right] \quad (10)$$

where F is the free energy of the system excluding the configurational entropy

$$F = E + A_v \quad (11)$$

All of the regular solution based models of segregation are based upon approximations to the heat of segregation $Q_n(= \partial F/\partial C_n - \partial F/\partial C_B)$. For example, the Langmuir, McLean formula is derived on the basis of first-layer segregation, with noninteracting segregants and equivalent segregation sites, i.e., the heat of segregation Q_1 is a *constant*. Our results for Q_1 (evaluated as $\partial F/\partial C_1 - \partial F/\partial C_B$) at $T = 600$ K are plotted as a function of the bulk concentration, C_B, in figure 8 (solid lines). In all the three alloy systems, we find that Q_1 is not constant. This suggests that the Langmuir, McLean formula is not a very good approximation to the surface segregation results obtained in the present study.

However, the heat of segregation determined using equation (4) yields reasonable agreement with our results (see the dotted lines in Fig. 8). To determine the heat of segregation using equation (4), two parameters must be determined: the regular solution parameter ω and the difference between the surface energies in the pure systems. The surface energy difference was determined by performing simulations in the pure systems. The regular solution parameter is somewhat more complicated, and is evaluated by replacing one atom of a perfect A crystal with a B atom and then calculating the difference of the energy between these two crystals. If the atoms interact with nearest neighbor pair interactions, that difference is roughly equal to $12(\varepsilon_{AB} - \varepsilon_{AA})$. Similarly, by replacing one atom of the perfect crystal B with an A atom we obtain $12(\varepsilon_{AB} - \varepsilon_{BB})$. The addition of these two differences divided by 24 is an estimate of ω. Using this approach with the EAM potentials employed in the present study, we find, at $T = 0$ K, $\Delta(\gamma\sigma) = -0.0825\ eV$/atom

and $\omega = 0.0046$ eV for Cu-Ni alloys, $\Delta(\gamma\sigma) = -0.167$ eV/atom and $\omega = -0.0102$ eV for Au-Pd alloys, and $\Delta(\gamma\sigma) = 0.11$ eV/atom and $\omega = -0.0087$ eV for Au-Ag alloys. The largest discrepancy between our simulation results and equation (4) occurs in the Cu-Ni system. This difference between our Cu-Ni Q_1 versus C_B curve and that obtained using equation (4) is nearly constant over the entire concentration region. Equation (4) under estimates the magnitude of the heat of segregation by 30–40%. In Ag-Au alloys, the agreement between our simulation and equation (4) is very good in Au-rich alloys; errors of up to $\sim$ 20% are found in Ag-rich alloys. The best agreement between simulation and equation (4) is obtained in the Au-Pd alloy system.

The excess concentration on the (100) surface produced by the heat of segregation from our simulation results (solid line) is plotted as a function of the bulk concentration at $T = 600$ K in figure 9 along with that determined using equations (4) (dotted line). Not surprisingly, the agreement between simulation and equation (4) is excellent in the Au-Pd and Ag-Au systems with substantial disagreement in the Cu-Ni system, especially in the Ni-rich alloys.

The elastic energy associated with differences in atomic size is not explicitly included in equation (4). However, in these three alloy systems, the elastic energy caused by distortion may not be very large, since the difference in atomic size between the two elements in each binary alloy system are small (Au-Pd shows the largest difference $\sim$ 4%).

The bond-breaking models represented by equations (2)–(4), suggests that the element with the lower sublimation energy will segregate to the surface. This is consistent with our observations for Cu-Ni and Ag-Au alloys. However, in Au-Pd alloys, the sublimation energy of Pd is slightly smaller than that of Au, but Au segregates to the (100) surface. The major difference between equation (4) and equations (2) and (3) is that equation (4) employs the surface energy difference rather than the sublimation energy difference, as in equation (2) and (3). The surface energy accounts for surface relaxation, interactions beyond the first nearest neighbors, many body effects, and some atomic size effects.

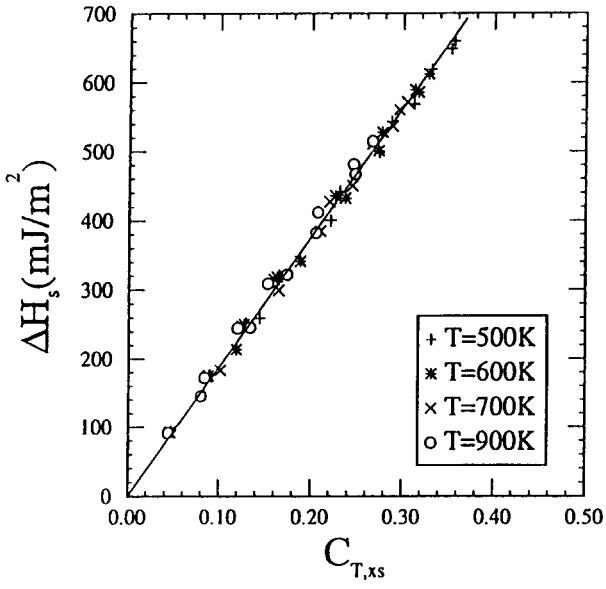

(*a*)

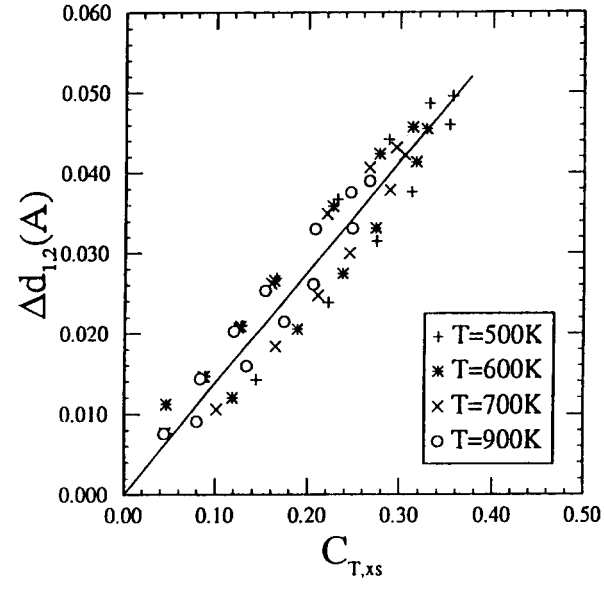

(*b*)

Fig. 7. (*a*) The excess surface enthalpy and (*b*) the excess separation between the first two (002) planes of Ag-Au alloys versus the total excess concentration. The straight lines are fit to all of the data.

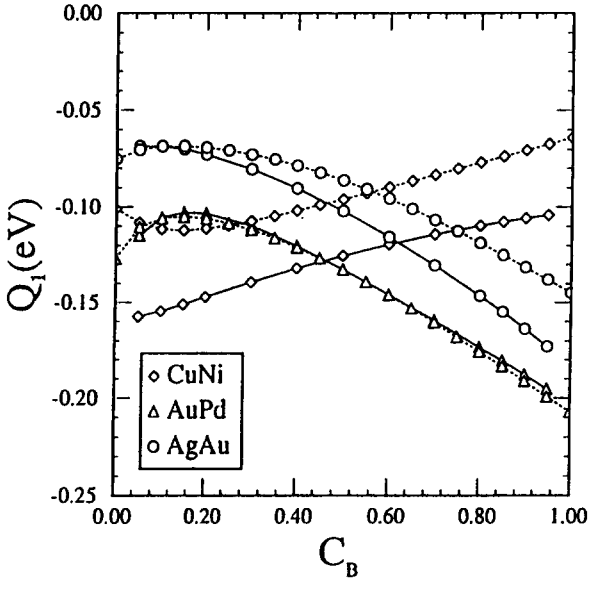

Fig. 8. The heat of surface segregation Q_1 versus the bulk concentration C_B. The solid line is calculated from our simulation by $\partial F/\partial C_1 - \partial F/\partial C_B$, and the dotted line is calculated by the classical theory equation (3). The diamond traingle, and circle are for Cu-Ni, Au-Pd, and Ag-Au alloys, respectively.

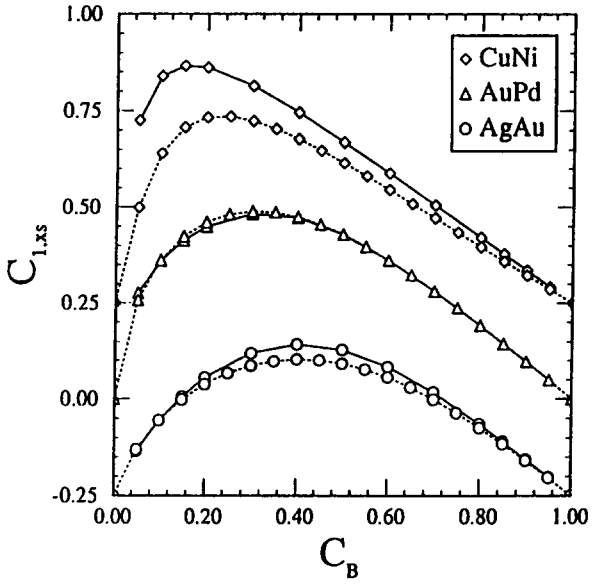

Fig. 9. The excess concentration of the first layer given by simulation (solid) and by equation (3) is plotted as a function of the bulk concentration. The diamond, triangle, and circle are for Cu-Ni, Au-Pd, and Ag-Au alloys, respectively. The excess concentration of Cu-Ni and Ag-Au alloys is displaced by 0.25 and −0.25, respectively.

This is consistent with the discussion of Abraham et al. [20–21], who noted that atoms with the lowest bond energy and the largest atomic surface area are more favorable to occupying surface positions. In Au-Pd alloys, Au has a slightly larger sublimation energy than Pd, but Au has a larger atomic size. This compensates for Au's larger sublimation energy producing a smaller surface energy for Au than Pd, which in turn favors Au segregation, as per equation (4).

In order to evaluate the degree to which relaxation, with respect to atomic position and concentration affect the heat of segregation, we calculated the heat of segregation in three different limits: (1) both the atomic concentrations and positions are relaxed; (2) only the atomic positions are relaxed; and (3) neither the atomic concentrations nor positions are relaxed. The heat of segregation in Cu-Ni alloys is plotted as a function of the bulk concentration in all three limits in figure 10(*a*). The three values are very close to each other, implying the relaxation with respect to atomic position and concentration is relatively unimportant. However, for Au-Pd and Ag-Au alloys (Fig.10(*b*)(*c*), the three values are quite different. This implies that relaxations are very important in these two alloys. For both Au-Pd and Ag-Au alloys, the relaxations reduce the magnitude of the heat of segregation. The heat of segregation of the compositionally unrelaxed surface lies between the values of Q_1 determined in the other two limits. Although in some cases, such as the (100) surface in Cu-Ni alloys, relaxation is not very important, in general, minimization of the free energy with respective to both the position and the concentration is necessary.

Several authors [11, 37–39] pointed out that when the regular solution parameter w is positive, the binary alloy system has the properties representative of a miscibility gap, and that this may lead to a form of clustering, in which the concentration profile exhibits a monotonic decay into the bulk. One the other hand, when w is negative, the system may tend to order, such that a change a segregant occurs at the second layer. In our simulations, only Ag-Au alloys

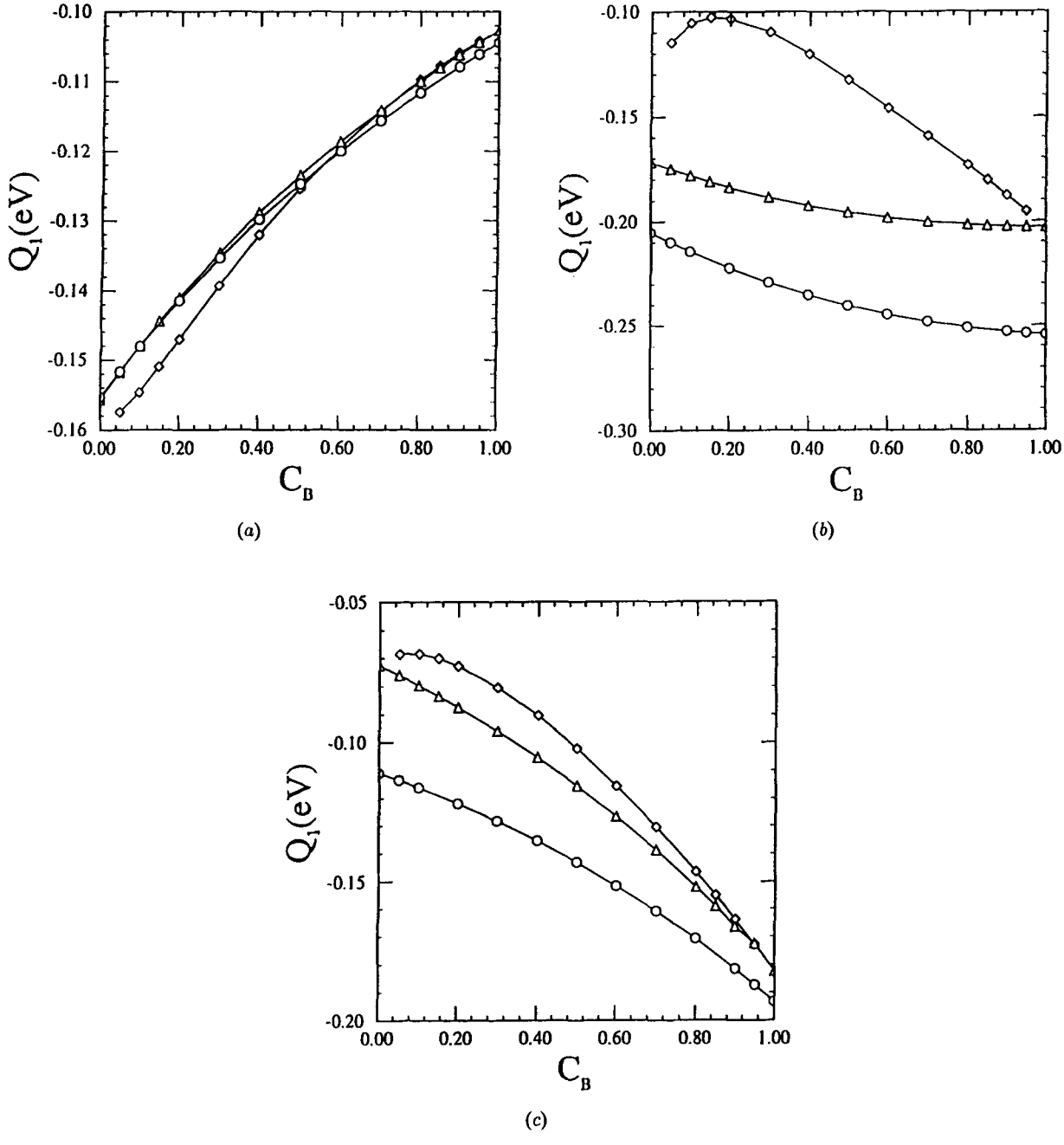

Fig. 10. The heat of surface segregation $Q_1(= \partial F/\partial C_1 - \partial F/\partial C_B)$ for the segregated surface (diamond), the unsegregated surface (triangle), and the unrelaxed surface (circle) versus the bulk concentration C_B with (*a*), (*b*), and (*c*) for Cu-Ni, Au-Pd, and Ag-Au alloys, respectively.

exhibit both a negative w and a change in segregant at the second layer. Au-Pd alloys also have a negative w, but the change in segregant does not occur until the third layer. Further, Cu-Ni alloys have a positive ω, such that a second layer change in segregant should not occur, but indeed show such a second layer change in segregant, in agreement with experimental results [40]. Ng attributes the presence of this change in segregant to surface relaxation [40] based upon his modeling results using the four-layer segregation model of Williams and Nason [11].

In figure 11, the heat of segregation for the second (002) layer Q_2 is plotted as a function of the bulk concentration based upon the relaxed (solid lines) and unrelaxed (dotted lines) surfaces. The data obtained based upon the unrelaxed surface agrees poorly with the more accurate data obtained from the relaxed surface. The heat of segregation of the second layer does not vary monotonically as the bulk composition is varied. This suggests that the variations of the composition of the second (002) layer with changes in the bulk composition will be complex. In fact, in the Ag-Au system, the second layer segregant will change from Ag near pure Au compositions to Au as the bulk Ag composition is increased. Since these data were obtained for the relaxed surface, these data suggests that neither the presence to surface relaxations or the value of w are sufficient to predict the qualitative form of the segregation profile.

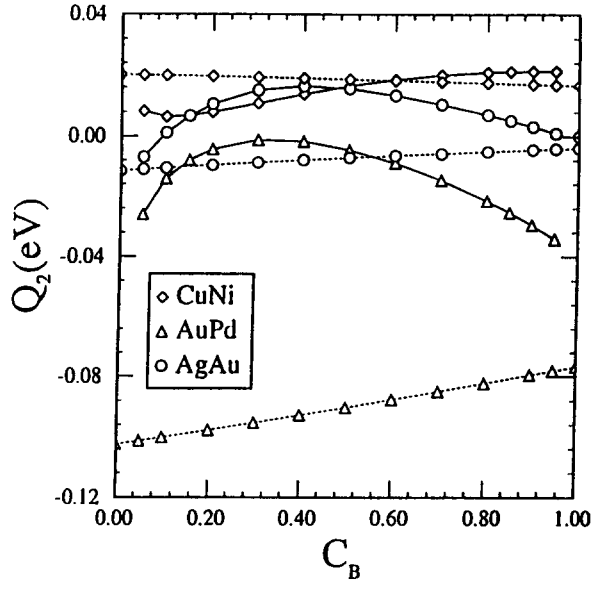

Fig. 11. The heat of segregation for the second (002) plane $Q_2(= \partial F/\partial C_2 - \partial F/\partial C_B)$ for the segregated surface (solid) and the unrelaxed surface (dotted) versus the bulk concentration C_B with diamonds, triangles, and circles for Cu-Ni, Au-Pd, and Ag-Au alloys, respectively.

5. Conclusions

Atomistic simulations of segregation to (100) free surface in Ag-Au, Au-Pd, and Cu-Ni alloy systems have been performed for a wide range of temperatures and compositions within the solid solution region of these alloy phase diagrams. In addition to the surface segregation profiles, surface free energies, enthalpies, and entropies were determined. These simulations were performed within the framework of the free energy simulation method, in which an approximate free energy functional is minimized with respect to atomic coordinates and atomic site occupation. The effects of the relaxation with respect to either the atomic positions or the atomic concentrations are discussed. For all alloy bulk compositions ($0.05 \leq C \leq 0.95$) and temperatures ($400 \leq T\,(\mathrm{K}) \leq 1,100$) examined, Ag, Au, and Cu segregate to the surface in the Ag-Au, Au-Pd, and Cu-Ni alloy systems, respectively. The present results are compared with several theories for segregation. The resultant segregation profiles in Au-Pd and Ag-Au alloys are shown to be in good agreement with an empirical segregation theory, while in Cu-Ni alloys the disagreement in Ni-rich alloys is substantial. The width of the segregation profile is limited to approximately three to four atomic planes. The surface thermodynamic properties depend sensitively on the magnitude of the surface segregation, and some of them are shown to vary linearly with the magnitude of the surface segregation.

Acknowledgment

We gratefully acknowledge the Division of Materials Science of the Office of Basic Energy Sciences of the United States Department of Energy

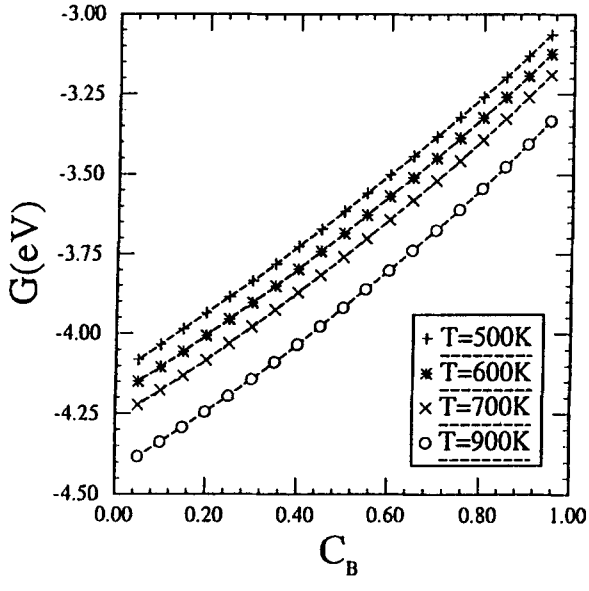

(*a*)

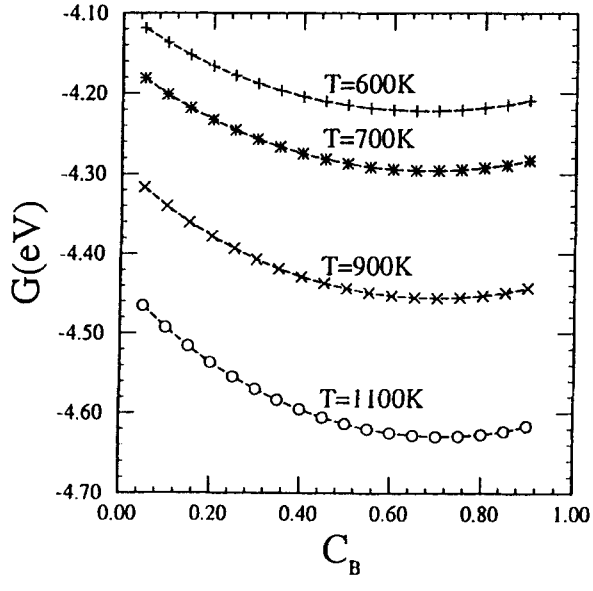

(*b*)

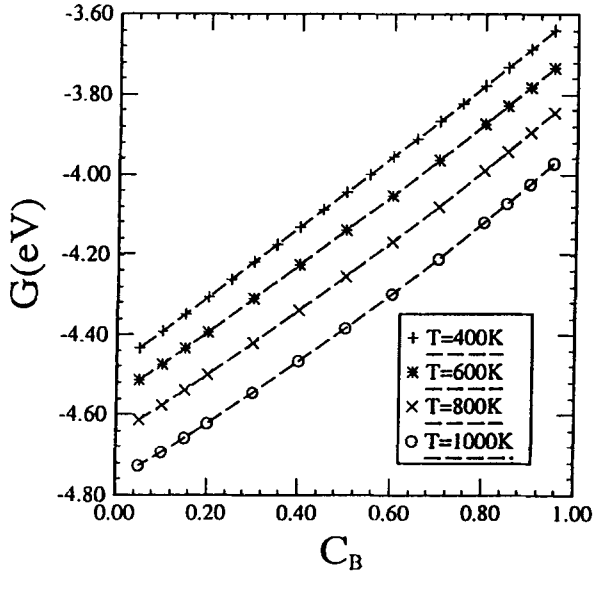

(*c*)

Fig. A1. The free energy of the perfect crystal G versus concentration: (*a*), (*b*), and (*c*) are for Cu-Ni, Au-Pd, and Ag-Au alloys, respectively.

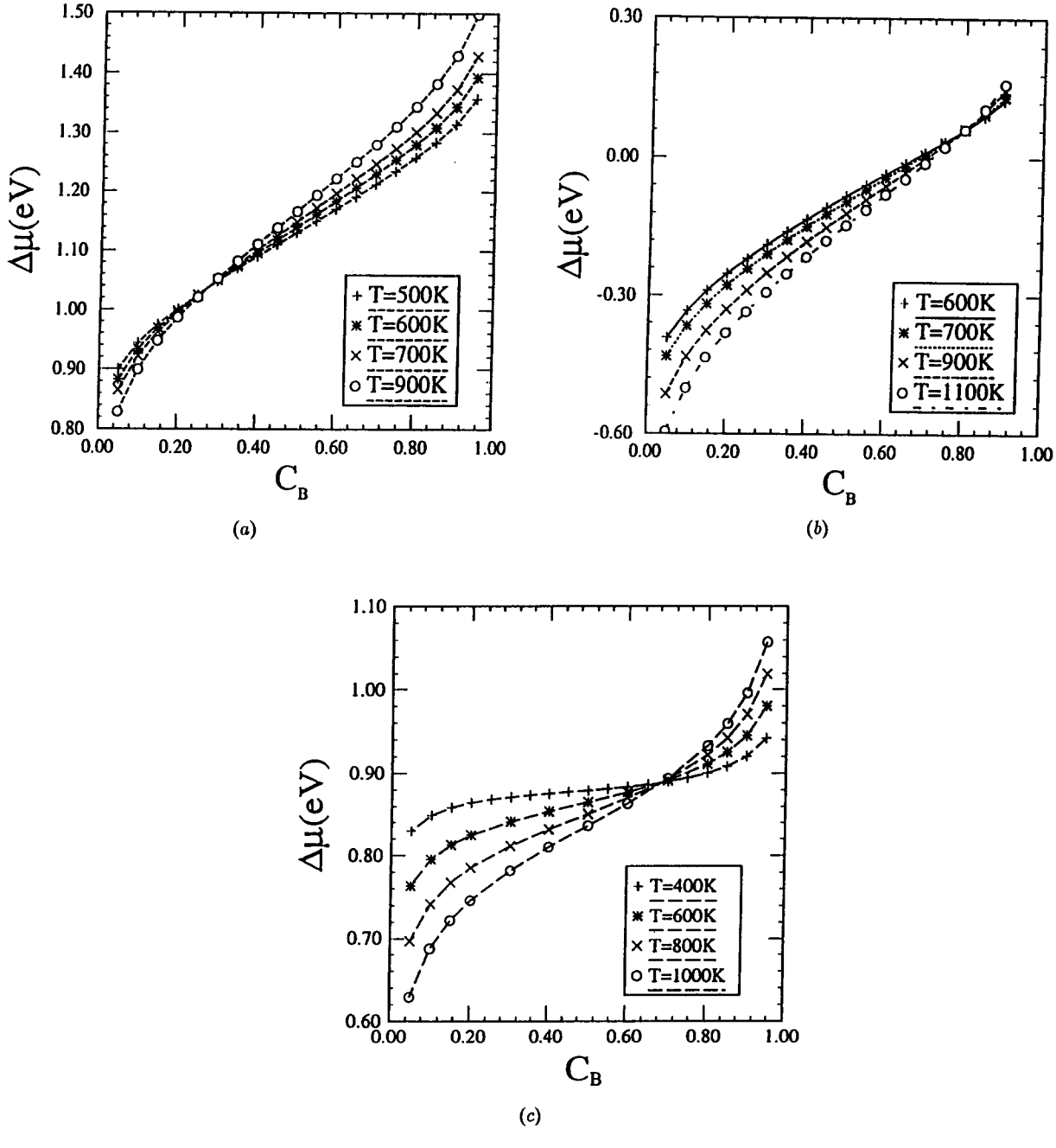

Fig. A2. The chemical potential difference between the two elements in the alloys versus concentration (*a*), (*b*), and (*c*) are for Cu-Ni, Au-Pd, and Ag-Au alloys, respectively.

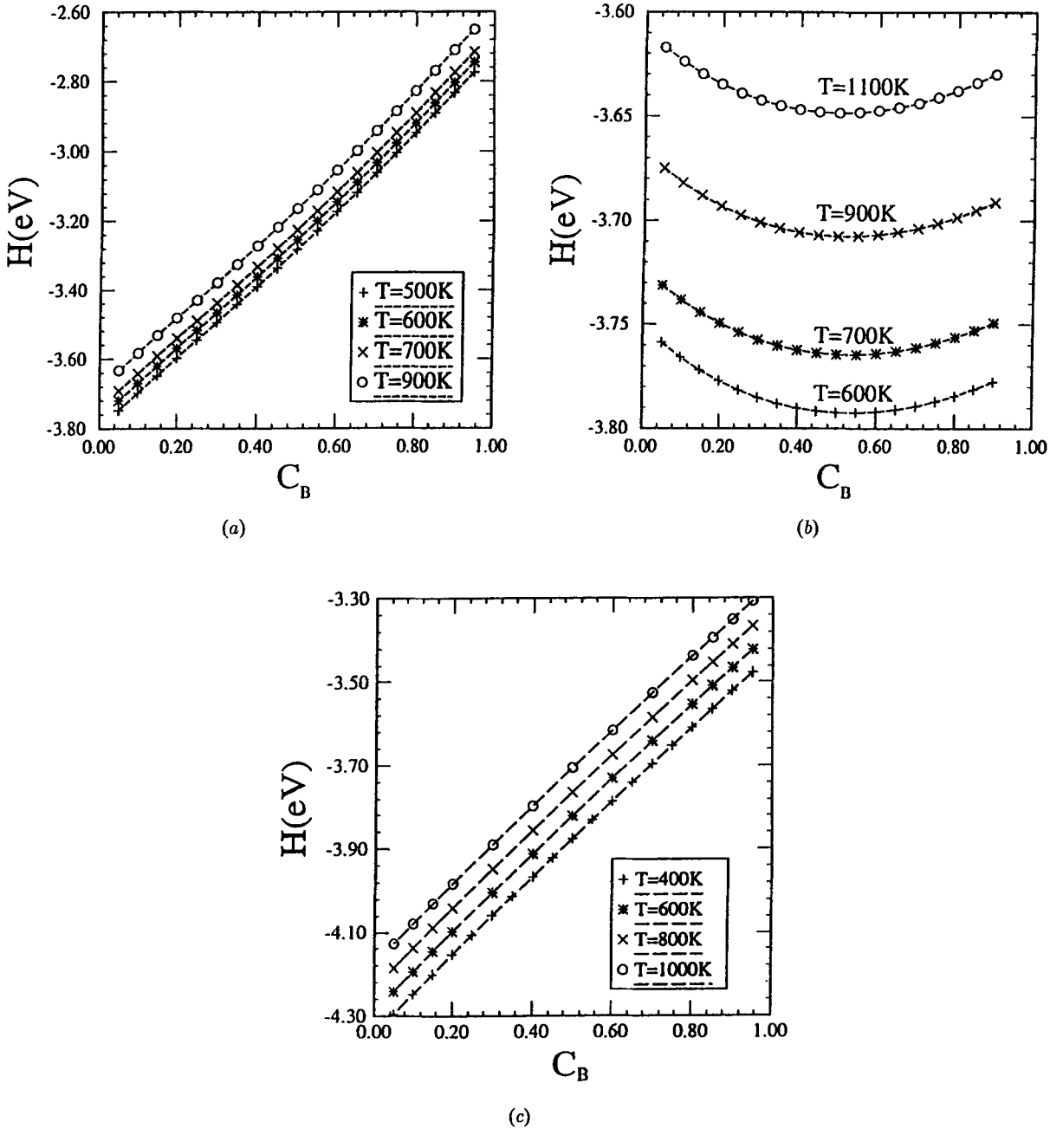

Fig. A3. The enthalpy of the perfect crystal versus concentration: (*a*), (*b*), and (*c*) are for Cu-Ni, Au-Pd, and Ag-Au alloys, respectively.

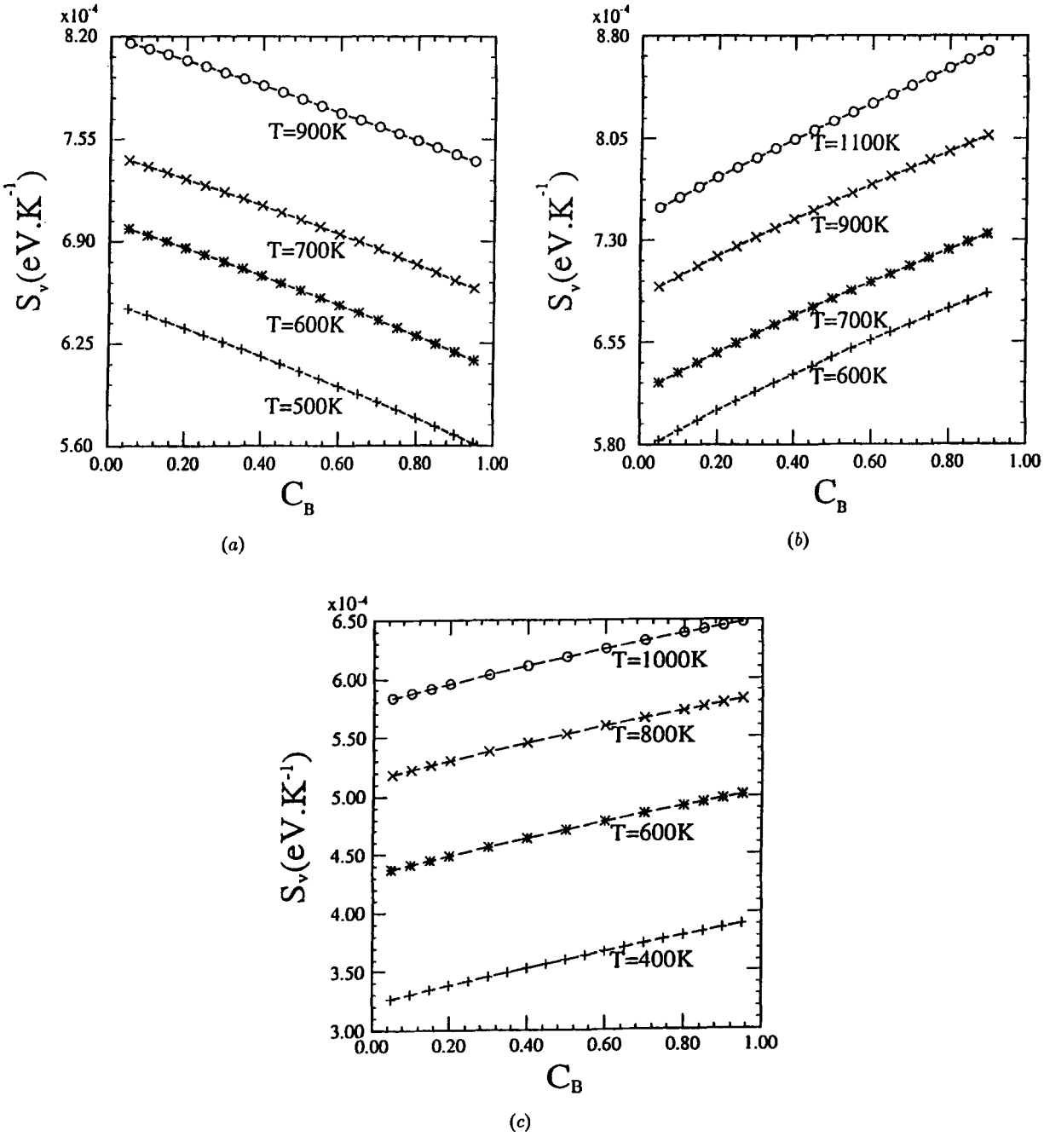

Fig. A4. The vibrational entropy of the crystal versus concentration: (*a*), (*b*), and (*c*) are for Cu-Ni, Au-Pd, and Ag-Au alloys, respectively.

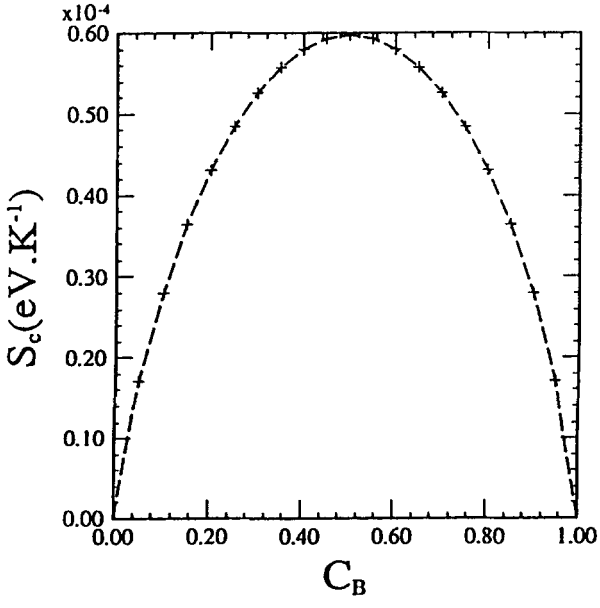

Fig. A5. The configurational entropy of the perfect crystal versus concentration.

(DOE BES DMS), Grant #FG02-88ER45367 for its support of this work. The work of R. LeSar was performed under the auspices of the U.S. Department of Energy and also supported, in part, by DOE BES DMS.

Appendix

Before the structure, segregation and properties of surfaces in Ag-Au, Au-Pd, and Cu-Ni alloys can be examined, it is first necessary to determine the properties of perfect crystals in these alloy systems. We determined the structure and properties of perfect solid solution Ag-Au, Au-Pd, and Cu-Ni crystals by minimizing the grand potential at fixed values of temperature, concentration and pressure. In the present calculations, we fixed the external pressure at zero. The composition was fixed in terms of the chemical potential difference between the elements in the alloys. Since the only crystalline structure that occurs in the Ag-Au, Au-Pd, and Cu-Ni phase is the face center cubic structure, the grand potential minimization was performed with respect to the single lattice parameter.

All the thermodynamic properties are plotted as functions of Cu, Au, or Ag concentration, depending on whether the alloys is Cu-Ni, Au-Pd, or Ag-Au, respectively. The Gibbs free energy G of four different temperatures are plotted in Fig. A1. The free energy of Cu-Ni alloys (Fig. A1(a) and Ag-Au alloys (Fig. A1(c) are monotonically increasing with increasing Cu and Ag concentration, respectively; for Au-Pd (Fig. A1(b), the free energy has a minimum. For all the three alloys, the free energy increases with decreasing temperature. Concentration is varied in these simulations by changing the chemical potential difference $\Delta\mu = -\partial G/\partial C_B$. The relationship between concentration and $\Delta\mu$ is nonlinear, as shown in figure A2. The slopes of the curves in these plots increase with increasing temperature and become horizontal in the limit that T goes to zero due to the requisite zero solubility at zero temperature.

The enthalpy H is plotted as a function of bulk concentration in figure A3. The enthalpy H is equal to the total internal energy, since the simulations were performed at zero pressure, and is equal to the potential energy plus $3k_BT$. The $3k_BT$ comes from the vibrational energy within the classical approximation. The enthalpy varies in a nearly linear manner as the concentration is changed from pure Ni to pure Cu for the Cu-Ni alloys (Fig. A3(a) and from pure Au to pure Ag for the Ag-Au alloys (Fig. A3(c)). For Au-Pd alloys, again the enthalpy has a minimum, and the curves have a relatively higher curvature than that of Cu-Ni and Ag-Au alloys. For all the three cases, increasing temperature simply shifts the enthalpy versus C_B curves to higher enthalpy.

The entropy consists of two parts: vibrational and configurational. The vibrational entropy S_v is plotted against the bulk concentration C_B in figure A4. The vibrational entropy varies with increasing C_B in a nearly linear manner, and increasing temperature simply shifts these curves to higher entropy. The concentration dependence of the configurational entropy S_c is shown in figure A5. Within the simple-point approximation employed within the present simulations, S_c is simply a function of concentration, and is independent of atom type or temperature.

References

1. R. Najafabadi, H.Y. Wang, D.J. Srolovitz, and R. LeSar, Acta Metall. Mater. 39, 3071 (1991); Mat. Res. Soc. Symp. Proc. **213**, 51 (1991).
2. H.Y. Wang, R. Najafabadi, D.J. Srolovitz, and R. LeSar, Mat. Res. Soc. Symp. Proc. **209**, 219 (1991).
3. H.Y. Wang, R. Najafabadi, D.J. Srolovitz, and R. LeSar, Phil. Mag. **65**, 625 (1992).
4. H.Y. Wang, R. Najafabadi, D.J. Srolovitz, and R. LeSar, Phys. Rev. B **45**, 12028 (1992).
5. J.W. Gibbs, *Collected Works*, vol. I (Yale University Press, New Haven, CT, 1948).
6. T.M. Buck, in *Chemistry and Physics of Solid Surfaces IV*, edited by K. Vanselow and R. Howe (CPC Press, Boca Raton, FL, 1982), p. 435.
7. T.S. King, in *Surface Segregation Phenomena*, edited by P.A. Dowben and A. Miller (CRC Press, Boca Raon, FL, 1990), p. 27.
8. P. Wynblatt and K.C. Ku, in *Interfacial Segregation*, edited by W.C. Johnson and J.M. Blakely (American Society for Metals, Metal Park, Ohio, 1979), p. 115.
9. D. McLean, *Grain Boundaries in Metals* (Clarendon Press, Oxford, 1957).
10. R. Defay, I. Prigogine, A. Bellemans, and D.H. Everett, *Surface Tension and Adsorption* John Wiley and Sons, New York, 1966), p. 158.
11. F.L. Williams and D. Nason, Surf. Sci. **45**, 377 (1974).
12. H.H. Brongersma, M.J. Sparnay, and T.M. Buck, Surf. Sci. **71**, 657 (1978).
13. V. Kumar, D. Kumar, and S.K. Joshi, Phys. Rev. B **19**, 1954, (1979).
14. V. Kumar, Phys, Rev. B **23**, 3756 (1981).
15. H.H. Brongersma and T.M. Buck, Surf. Sci. **53**, 649 (1975).
16. P. Wynblatt and R.C. Ku, Surf. Sci. **65**, 511 (1977).
17. J. Friedel, Advan. Phys. **3**, 446 (1954).
18. M.A. Hoffmann and P. Wynblatt, Surf, Sci. **236**, 369 (1990).
19. F.F. Abraham, N.H. Tsai, and G.M. Pound, Surf. Sci. **83**, 406 (1979).
20. F.F. Abraham, Phys. Rev. Lett. **46**, 546 (1981).
21. F.F. Abraham and C.R. Brundle, J. Vac. Sci. Technol. **18**, 506 (1981).
22. J.J. Burton and E.S. Machlin, Phys Rev. Lett. **37**, 1433 (1976).
23. J.K. Strohl and T.S. King, J. Catal, **118**, 53 (1984).
24. T.S. King, in *Surface Segregation Phenomena*, edited by P.A. Dowben and A. Miller (CRC Press, Boca Raton, FL, 1990), p. 27.
25. S.M. Foiles, Phys, Rev. **B32**, 7685 (1985).
26. S.M. Foiles, Phys, Rev. **B40**, 11502 (1989).
27. Y.S. Ng., T.T. Tsong, and S.B. McLane Jr., J. Appl. Phys. **51**, 6189 (1980).
28. Toshio Sakurai, T. Hashizume, A. Jimbo, A. Sakai, and S. Hyodo, Phys. Rev. Lett. **55**, 514 (1985).
29. Toshio Sakurai, T. Hashizume, A. Kobayashi, A. Sakai, and S. Hyodo, Y. Kuk, and H.W. Pickering, Phys. Rev. **B34**, 8379 (1986).
30. M.S. Daw and M.I. Baskes, Phys. Rev. Lett. **50**, 1285 (1983).
31. M.S. Daw and M.I. Baskes, Phys. Rev. **B29**, 643 (1984).
32. S.M. Foiles, M.I. Baskes, and M.S. Daw, Phys. Rev. **B33**, 7983 (1986).
33. R. LeSar, R. Najafabadi, and D.J. Srolovitz, Phys. Rev. Lett. **63**, 624 (1989).
34. R. Najafabadi, D.J. Srolovitz, and R. LeSar, J. Mat. Res. **5**, 2663 (1990).
35. K. Huang, *Statistical Mechanics* (John Wiley and Sons, Inc., New York, 1963).
36. W.E. Press, B.P. Flannery, S.A. Teukolsky, and W.T. Vetterling, *Numerical Recipes* (Cambridge University Press, Cambridge, 1986).
37. F.L. Williams and D. Nason, Surf. Sci. **45**, 377 (1974).
38. S. Hoffmann, in *Surface Segregation Phenomena*, edited by P.A. Dowben and A. Miller (CPC Press, Boca Raton, FL, 1990), p. 107.
39. M. Guttmann and D. McLean, in *Interfacial Segregation*, edited by W.C. Johnson and J.M. Blakely (American Society for Metals, Metal Park, Ohio, 1979), p. 261.
40. M. Militzer and J. Wieting, Acta Mettll. **35**, 2765 (1987).
41. Y.S. Ng, T. T. Tsong, and S.B. McLean Jr., Phys Rev. Lett. **42**, 588 (1979).